



# A nondestructive guided wave propagation method for the characterization of moisture-dependent viscoelastic properties of wood materials

Hamidreza Fathi · Siavash Kazemirad · Vahid Nasir

Received: 22 July 2020 / Accepted: 2 November 2020 / Published online: 26 November 2020  
© RILEM 2020

**Abstract** The in-situ monitoring and characterization of the mechanical properties of wood and timber materials is of great importance due to their broad structural applications. The purpose of this study was to propose a nondestructive method to assess the moisture-dependent viscoelastic behavior of structural wood using the guided Lamb wave propagation. Twelve green poplar wood specimens with different moisture content (MC) underwent the Lamb wave propagation tests and the wave characteristics were acquired. The viscoelastic properties of the wood specimens, including the shear storage and shear loss moduli and the loss factor, were then estimated through the solution of the corresponding inverse Lamb wave propagation problem using the experimentally measured Lamb wave characteristics. The structural stiffness and damping of wood specimens were affected by their MC, as the Lamb wave amplitude and velocity significantly decreased with MC. While the shear storage modulus decreased with MC, the shear loss modulus and loss factor increased with MC, resulting in a higher viscoelastic behavior. The loss factor of the wood specimens was estimated

to be between 5.88% and 8.49% for different classes of MC, showing an increase of 44% with MC. The Lamb wave propagation method offers a strong tool for nondestructive characterization of the viscoelastic properties of wood materials and structures over a broad MC range. Wood materials show a significant viscoelastic behavior which is highly impacted by their MC. The loss factor can play an important role in the characterization and classification of structural wood and timber with different MC.

**Keywords** Viscoelastic properties · Natural materials · Materials characterization · Lamb wave · Nondestructive evaluation · Ultrasound

## 1 Introduction

Wood materials are being extensively used in different structural applications, Therefore, the in-situ nondestructive characterization of the mechanical properties of structural wood is of great importance for health monitoring and quality control purposes. Besides, wood is known to be a viscoelastic natural material. Thus, the viscoelasticity assessment of wood materials is needed to fully comprehend the behavior of load-carrying wood structures in different conditions. Destructive methods, including the tensile and bending tests, are mainly used to obtain the mechanical

---

H. Fathi · S. Kazemirad (✉)  
School of Mechanical Engineering, Iran University of  
Science and Technology, Tehran 16846-13114, Iran  
e-mail: skazemirad@iust.ac.ir

V. Nasir  
Centre for Advanced Wood Processing, The University of  
British Columbia (UBC), Vancouver, Canada



properties of balk wood and wood-based composites [1, 2]. Such methods are, however, time-consuming and cannot be used for the on-line characterization of material properties. On the other hand, the natural variations, complex anatomy, and behavior of wood have made it difficult to propose an accurate nondestructive evaluation (NDE) method for the characterization of the mechanical properties of wood materials [3, 4].

The viscoelastic properties of wood materials have been assessed using different methods in the literature [5–12]. For example, Hering and Niemz [8] used the four-point bending tests to investigate the moisture dependent creep compliance of European beech wood. Dubois et al. [9] presented a rheological model based on the generalized Kelvin-Voigt model for describing the viscoelastic properties of wood. They performed longitudinal tensile creep tests on Douglas fir specimens for verification purposes. Ozyhar et al. [10] investigated the time-dependent viscoelastic behavior of beech wood by performing the tensile and compression creep experiments in different wood's orthotropic directions. Li et al. [12] assessed the temperature-dependent viscoelastic properties of Chinese fir wood using dynamic mechanical analysis. The strain-rate dependent behavior of wood, which is related to its viscoelastic behavior, has also been investigated in prior research studies [13]. However, in all of the mentioned studies, the characterization of the viscoelastic properties of wood has been performed using destructive methods. Therefore, the reliable nondestructive quantification of the viscoelastic properties of wood materials is yet to accomplish.

Near-infrared (NIR) spectroscopy [14–16] and the ultrasonic and stress wave methods [17–22] have been widely used in the literature for nondestructive characterization of wood materials. To the authors' knowledge, none of these methods has been used for the assessment of the viscoelastic properties of wood materials. NIR spectroscopy has been mainly used for the estimation of the modulus of elasticity (MOE) and the density of wood [16]. The NIR spectroscopy was, however, shown to face challenges including the need for frequent calibration and the accuracy issue in the case of the characterization of thick timbers [16]. The ultrasonic and stress wave methods have been extensively used for the estimation of the dynamic MOE ( $MOE_d$ ) of wood materials through the measurement of the ultrasonic wave velocity [3, 17]. However, it

was shown that the relation between the MOE and  $MOE_d$  depends on different factors including the wood species type and moisture content (MC) [23, 24], and the  $MOE_d$  overestimates the static MOE, especially at high MC levels [25, 26]. Therefore, not only there is currently a knowledge gap for nondestructive characterization of the viscoelastic properties of wood materials, but the accurate nondestructive estimation of their elastic properties has remained challenging.

Guided wave propagation methods have been extensively used for the evaluation of materials and structures, and damage detection purposes [27–32]. Guided waves that propagate in plate-like media are called Lamb waves [33], which may be used for nondestructive characterization of the properties of wood materials. For example, Dahmen et al. [27] assessed the elastic properties of olive wood plates using the Lamb and bulk ultrasonic wave propagation methods. Yang et al. [29] examined the Lamb wave propagation in a woven glass fiber/epoxy composite laminate to identify and localize a circle through-hole defect in it. As the characteristics of Lamb wave, including the wave velocity and displacement amplitude, are related to the mechanical properties of the propagation medium, the Lamb wave propagation has become an ideal choice for nondestructive evaluation of the mechanical properties of different types of materials. Besides, the low attenuation nature of Lamb waves makes it suitable for fast and in-situ characterization of large structures. This may be regarded as an important issue for health monitoring and quality control purposes. Furthermore, the application of different Lamb wave modes and excitation frequencies allows the detection of a variety of tiny internal defects embedded in the material under investigation. However, despite the broad application of the Lamb wave propagation for materials evaluation and damage detection purposes, far less attention has been paid in prior research studies to the characterization of the mechanical properties of wood materials and timber structures using this method. For example, Fathi et al. [34] have recently proposed a machine learning-based model for predicting the MOE and modulus of rupture (MOR) of wood using the guided Lamb wave method. Besides, there is a knowledge gap in the literature regarding the nondestructive investigation of the shear storage and loss moduli of wood materials. These are crucial viscoelastic properties [35], through which the loss factor



is calculated that indicates the inherent viscoelasticity of a material. While these parameters have been widely investigated in the literature for the characterization of different constructional materials [32], less attention has been given to the assessment of the shear storage and loss moduli of structural wood.

This study aimed to propose a nondestructive Lamb wave propagation method for the assessment of the moisture-dependent viscoelastic properties of wood materials. The main hypothesis was that the Lamb wave characteristics can be properly related to the viscoelastic properties of wood at varying MC, and thus the Lamb wave propagation method can offer an accurate and reliable tool for the estimation of the shear storage and shear loss moduli and the loss factor of wood materials. The analytical model for the inverse problem of Lamb wave propagation in viscoelastic media is presented, in which the input parameters are the experimentally measured Lamb wave velocity and the decay of displacement amplitude with the propagation distance. Green wood specimens were used to evaluate the performance of the proposed method for the estimation of the viscoelastic properties of wood over a broad MC range. To evaluate the proposed method, the elastic storage modulus obtained from the nondestructive Lamb wave propagation tests was compared with the elastic modulus obtained from the destructive mechanical three-point bending tests.

## 2 Lamb wave propagation in viscoelastic materials

Lamb waves are produced in plate-like structures by the interaction of compression and shear waves near the two stress-free boundaries of such structures (Fig. 1). Lamb waves have two different modes of propagation, namely the symmetric and antisymmetric modes, defined based on the variations of displacement and stress fields through the structure thickness. Lamb waves are dispersive, meaning that the velocity of different Lamb wave modes varies with the wave frequency. In order to properly characterize the mechanical properties of materials with different geometrical dimensions and mechanical properties, the appropriate propagation mode and frequency should be selected.

The structural wood material investigated in this study were assumed to be linear viscoelastic,

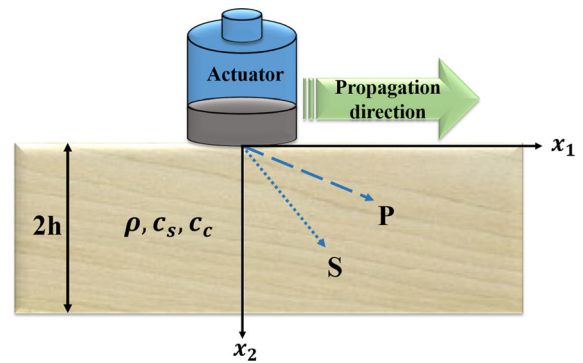


**Fig. 1** Schematic of the Lamb wave propagation concept. The interaction of compression (P) and shear (S) waves near the stress-free boundaries of a plate-like structure results in the Lamb wave propagation

macroscopically homogeneous, and isotropic in the wave propagation direction. As very small deformations are induced in the specimens during the Lamb wave propagation tests, the assumption of linear viscoelasticity may be generally valid. The assumption of being macroscopically homogeneous and isotropic may also be valid for the wood materials when their internal microscopic inhomogeneities are smaller than the wavelength and their material properties do not change significantly in the wave propagation direction. Considering such assumptions, the correspondence principle for linear viscoelasticity was used in this study. Consequently, the wave motion in a linear viscoelastic, macroscopically homogeneous, and isotropic material is governed by the Navier equation [33]. The decomposition of the displacement vector in the Navier equation using the compression and shear wave potentials, application of the proper boundary conditions, and simplification of the equations leads to the following equation for the antisymmetric Lamb wave propagation in viscoelastic media [32]:

$$\frac{\tanh(\hat{\eta}h)}{\tanh(\hat{\gamma}h)} = \frac{4k_T^2 \hat{\eta} \hat{\gamma}}{(2k_T^2 - k_S^2)^2} \quad (1)$$

where  $\hat{\eta}$  and  $\hat{\gamma}$  are defined as:

$$\hat{\eta}^2 = k_T^2 - k_c^2 \quad (2)$$

$$\hat{\gamma}^2 = k_T^2 - k_s^2 \quad (3)$$

and  $\hat{k}_l$ ,  $\hat{k}_c$ , and  $\hat{k}_s$  are the complex Lamb, compression, and shear wavenumbers, respectively, which are expressed as [32]:

$$\hat{k}_l(\omega) = \alpha(\omega) - i\beta(\omega) = \frac{\omega}{c_l} - i\beta(\omega) \quad (4)$$

$$\hat{k}_c(\omega) = \frac{\omega}{\sqrt{(\hat{\lambda} + 2\hat{\mu})/\rho}} \quad (5)$$

$$\hat{k}_s(\omega) = \frac{\omega}{\sqrt{\hat{\mu}/\rho}} \quad (6)$$

Furthermore, the shear wave velocity ( $c_s$ ) is related to the compression wave velocity ( $c_c$ ) via:

$$\left(\frac{c_s}{c_c}\right)^2 = \frac{1-2\nu}{2-2\nu} \quad (7)$$

in which  $\nu$  is the Poisson's ratio. The following equation can be used to obtain the imaginary part of the Lamb wavenumber ( $\beta(\omega)$ ) based on the displacement component along the  $x_2$  direction on the top surface of the plate-like material at two different locations along the propagation direction ( $x_1$ ), with a distance  $L$  from each other [32]:

$$\frac{\|\hat{u}_2(x_1^2, \omega)\|}{\|\hat{u}_2(x_1^1, \omega)\|} = e^{\beta(\omega)L} \quad (8)$$

where  $\|\ \|\$  indicates the absolute value of a complex number. The complex shear wavenumber,  $\hat{k}_s(\omega) = \alpha_s(\omega) - i\beta_s(\omega)$ , is then calculated through the numerical solution of Eq. (1) using the obtained complex Lamb wavenumber. Furthermore, the complex shear modulus may be defined as follows:

$$\hat{G}_l(\omega) = G'_l(\omega) + iG''_l(\omega) \quad (9)$$

The complex shear modulus is also related to the complex shear wavenumber through the following expression:

$$\hat{G}_l(\omega) = \frac{\rho\omega^2}{k_s^2} \quad (10)$$

The shear storage and shear loss moduli and the loss factor ( $\eta$ ) of the propagation medium are consequently obtained via:

$$G'_l(\omega) = \rho\omega^2 \frac{\alpha_s^2(\omega) - \beta_s^2(\omega)}{[\alpha_s^2(\omega) + \beta_s^2(\omega)]^2} \quad (11)$$

$$G''_l(\omega) = 2\rho\omega^2 \frac{\alpha_s(\omega)\beta_s(\omega)}{[\alpha_s^2(\omega) + \beta_s^2(\omega)]^2} \quad (12)$$

$$\eta = \tan \delta = \frac{G''_l(\omega)}{G'_l(\omega)} = \frac{2\alpha_s(\omega)\beta_s(\omega)}{\alpha_s^2(\omega) - \beta_s^2(\omega)} \quad (13)$$

To verify the Lamb wave propagation method for the estimation of the viscoelastic properties of wood, the elastic storage modulus ( $E'_l$ ), which is considered as the stiffness of a viscoelastic material, was calculated using the estimated shear storage modulus and compared with the elastic modulus obtained from three-point bending tests. Based on the assumptions of the Lamb wave propagation presented above that considered the material to be linear viscoelastic, macroscopically homogeneous, and isotropic in the wave propagation direction, the elastic storage modulus is obtained via [32]:

$$E'_l = 2(1 + \nu)G'_l \quad (14)$$

in which  $G'_l$  denotes the shear modulus in the propagation plane. For example, if the Lamb wave is propagated in the longitudinal-tangential (L-T) plane of the specimens,  $G'_l$  is the shear storage modulus of the L-T plane ( $G'_{lLT}$ ). In this case,  $\nu_{LT}$  is used in Eq. (14) and the calculated elastic storage modulus is that in the longitudinal direction ( $E'_{lL}$ ). The Poisson's ratio of the specimens in the L-T plane ( $\nu_{LT}$ ) was measured through the compression testing similar to that performed in [36], and used for the estimation of the elastic storage modulus in the verification process.

### 3 Experimental procedure

#### 3.1 Materials

Twelve clear green poplar (*Populus x euramericana* (Dode) Guinier) wood specimens were prepared with the dimensions of  $2 \times 2 \times 30$  cm according to ISO-13061-3 and -4 in the longitudinal direction from flat



sawn poplar timbers obtained from a poplar tree grown in the Mazandaran province of Iran. With the intention of having specimens with various MC, they were cut and selected from different points along the stem. These specimens were used for the guided Lamb wave propagation and mechanical three-point bending tests. Cookies with a length of 5 cm and cross-section of  $2 \times 2$  cm were also cut from the vicinity of the main wood specimens to determine the corresponding MC and density of each specimen according to ISO-13061-1 and -2. The selected green wood specimens were defect-free without any knots and reaction wood. A flowchart showing the procedure of the Lamb wave propagation method and three-point bending tests is presented in Fig. 2.

### 3.2 MC and density measurements

The MC of wood specimens was measured using the oven-drying method according to ISO 13,061-1. The prepared cookies were initially weighted ( $m_1$ ) and then dried for 24 h in the oven at the temperature of  $103 \pm 2$  °C until they reached a constant mass ( $m_2$ ). The MC of each specimen was then calculated using the following relation:

$$W(\%) = \frac{m_1 - m_2}{m_2} \times 100 \quad (15)$$

in which  $m_1$ ,  $m_2$ , and  $W$  are the wet mass, dry mass, and MC of specimens, respectively. Moreover, the density ( $\rho_W$ ) of each specimen at the MC of  $W$  was obtained through:

$$\rho_W = \frac{m_W}{V_W} \quad (16)$$

where  $m_W$  and  $V_W$  are the mass and volume of specimens at the MC of  $W$ . After measuring the MC and density of specimens, the green wood specimens underwent the guided Lamb wave propagation and three-point bending tests.

### 3.3 Guided Lamb wave propagation tests

To obtain the viscoelastic properties of green wood specimens, the nondestructive guided Lamb wave propagation tests were performed. The viscoelastic properties of wood specimens were estimated through the analysis of acquired signals at different locations on the specimens. Figure 3 illustrates the experimental setup used for conducting the guided Lamb wave propagation tests. This setup consisted of a wave function generator (Owon AG1022F), digital oscilloscope (Owon TDS7104), computer, high power ultrasonic actuator, and high sensitivity ultrasonic sensor with a center frequency of 200 kHz.

An ultrasonic gel was used to ensure the proper coupling between the wood specimens and transducers. The choice of frequency is a trade-off between the wave attenuation (and thus propagation distance) and the sensitivity. While lower frequencies result in smaller attenuation of the wave amplitude with the propagation distance, higher frequencies allow the detection of tiny defects or minor variations in the structure and properties of the specimens. The frequency range of a few kHz is usually used for the

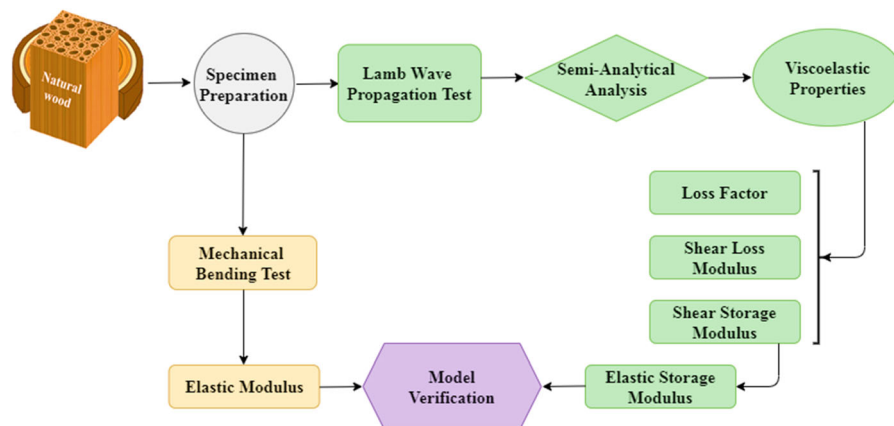


**Fig. 2** Flowchart of the procedure for quantifying the viscoelastic properties of green poplar wood specimens using the Lamb wave propagation method, and the verification using the three-point bending tests



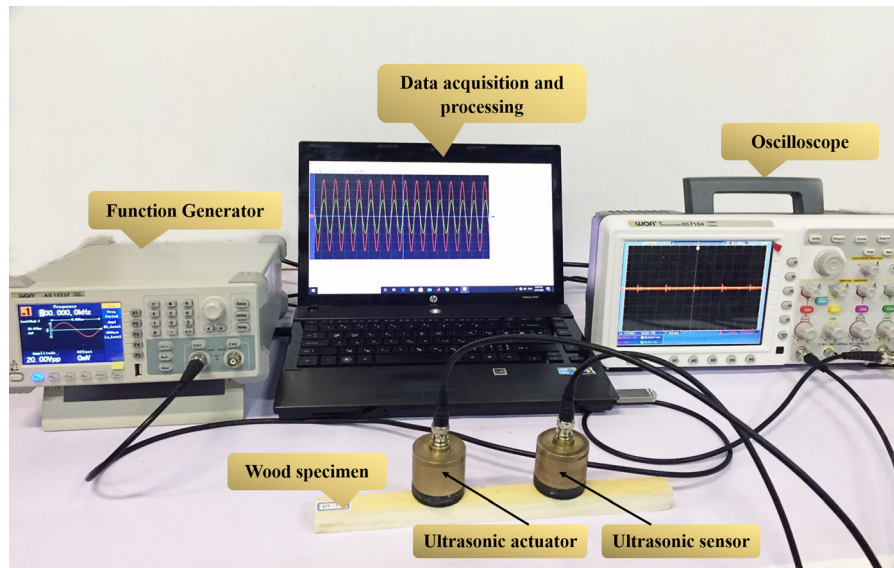


**Fig. 3** Guided Lamb wave propagation test setup

characterization and monitoring of materials and structures [27, 29], as this frequency range offers a good trade-off between the two mentioned issues. In the present study, a harmonic antisymmetric Lamb wave mode ( $A_0$ ) with a frequency of 200 kHz was generated in the L–T and longitudinal-radial (L–R) planes of the specimens using the actuator connected to the function generator. The propagated wave characteristics were acquired at four distances of 6, 8, 10, and 12 cm from the actuator using the sensor connected to the digital oscilloscope. A region in the middle of the specimens was selected to perform the Lamb wave propagation tests to avoid receiving the wave reflections from the sample boundaries in the acquired wave signals. All tests were performed with a constant sampling frequency of 10 Mega samples per second. The wave characteristics, including the phase and amplitude, were acquired at different actuator-sensor distances on the specimens. The acquired characteristics were analyzed using the analytical model of Lamb wave propagation in viscoelastic materials to assess the viscoelastic properties of wood specimens at different levels of MC.

### 3.4 Three-point bending tests

The schematic configuration of the mechanical three-point bending tests used for the verification of the results obtained from the proposed Lamb wave

propagation is shown in Fig. 4. Upon completing the guided Lamb wave propagation tests of each specimen, the mechanical test was performed on it according to ISO 13,061–3 and -4. A universal testing machine (STM-150, Santam Co.) with a crosshead speed of 1 mm/min was used for conducting the three-point bending tests. The wood specimens were kept in nylon packs to keep their MC almost constant prior to the bending tests.

The elastic modulus ( $E_m$ ) of the wood specimens were obtained using the mechanical three-point bending tests when the L–T plane of wood was under bending loading, which yielded the elastic modulus in the longitudinal direction,  $E_m = E_L$  [37]:

$$E_m = \frac{PL^3}{4bh^3f} \quad (17)$$

in which  $P$  and  $f$  represent the load equal to the difference between the upper and lower limits of loading and the corresponding difference between deflections of the upper and lower loading limits, respectively. Furthermore,  $L$ ,  $b$ , and  $h$  are the span length of the supports, breadth, and height of the specimens, respectively. Since the elastic storage modulus of the specimens estimated from the Lamb wave propagation tests was that of the longitudinal direction, it was comparable with the elastic modulus obtained from the bending tests.

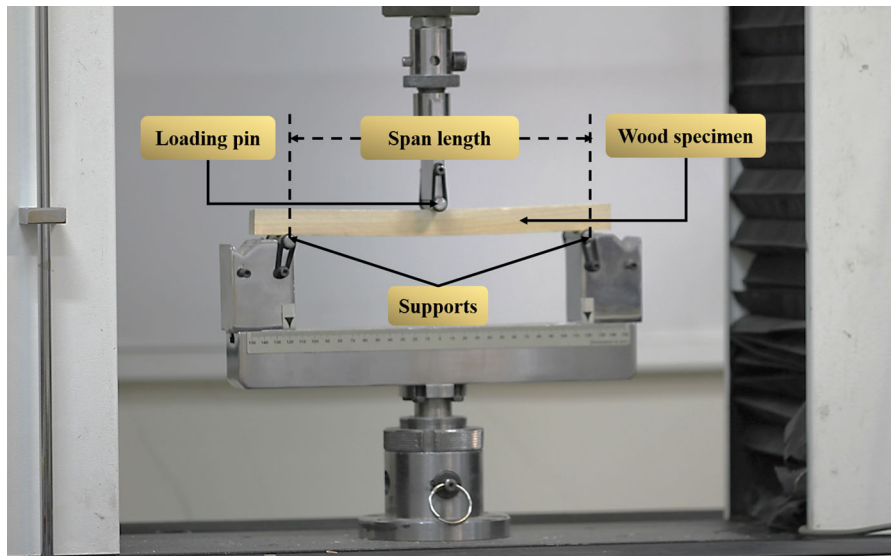


**Fig. 4** Mechanical three-point bending test setup

#### 4 Results and discussion

The results obtained from the MC and density measurements, and the guided Lamb wave propagation and mechanical three-point bending tests are presented and discussed in this section. The details of the physical properties of green poplar wood specimens obtained from the MC and density measurements are presented in Table 1. As revealed in this table, the MC of specimens was between about 50% and 130%. In order to investigate the effect of MC variation on the viscoelastic properties of wood specimens, the twelve specimens tested in this study were divided into three classes of MC each including four specimens, as seen in Table 1. It should be noted that the MC of none of the specimens was in the range between 70 to 80% and 100% to 120%.

The waveforms of the harmonic antisymmetric Lamb wave propagated in the wood specimens, for the three classes of MC, acquired at different actuator-

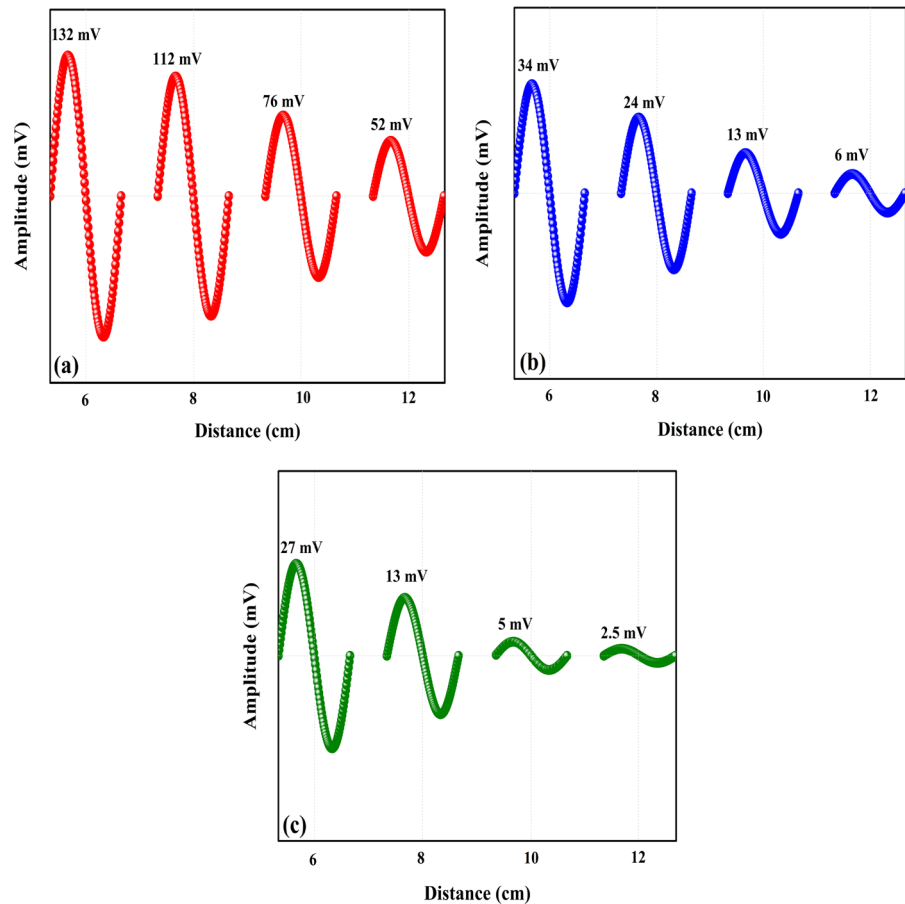
sensor distances are presented in Fig. 5. As shown in this figure, the acquired Lamb wave amplitude decreased with the propagation distance from the actuator. This indicates the dissipative behavior of the tested green wood specimens. It was also seen that the acquired Lamb wave amplitudes significantly decreased with MC, and this reduction is more pronounced at higher MC (Fig. 5). Therefore, it was revealed that the structural damping of wood specimens was highly related to the amount of water existing in them. This emphasizes the importance of the viscoelasticity assessment of wood materials while taking into account the impact of MC.

The ratio of Lamb wave amplitudes acquired at the actuator-sensor distances of 8, 10, and 12 cm to that of 6 cm, is shown in Fig. 6 for a typical wood specimen from each class of MC. Equation (8) was fitted to these amplitude ratios to obtain the imaginary part of the Lamb wavenumber. As seen, the Lamb wave amplitude ratio decreased nearly exponentially along the

**Table 1** The physical properties of green poplar wood specimens at different levels of MC

Class number	Number of specimens	MC (%)	Mean density (kg/m <sup>3</sup> )
1	4	50–70	572
2	4	80–100	655
3	4	120–130	839

**Fig. 5** The Lamb waveforms acquired at different actuator-sensor distances for **a** Class 1, **b** Class 2, and **c** Class 3 green poplar wood specimens



propagation direction. A comparison between this trend and what was previously given in Eq. (8) confirmed the presented analytical model for Lamb wave propagation in viscoelastic media.

The acquired Lamb wave signals were analyzed in the time domain and the Lamb wave velocity ( $c_l$ ) of each specimen was estimated using the phase difference of acquired signals at different locations along the propagation direction. The results (not presented here) revealed that the Lamb wave velocity did not vary significantly between the L–T and L–R planes. Thus, the average Lamb wave velocity measured in the two planes was selected as the Lamb wave velocity for each specimen. Finally, the mean value of measured Lamb wave velocities for the specimens of each class was considered as its Lamb wave velocity for the calculation of the mean Lamb wavenumber, shear wave velocity, and shear wavenumber of each class.

The mean Lamb and shear wave velocities and their corresponding wavenumbers obtained from the guided Lamb wave propagation tests for different classes of MC are reported in Table 2. As seen in this table, both of the Lamb and shear wave velocities decreased with MC, and the highest and lowest velocities belonged to Class 1 and Class 3, respectively. The decrease in both of the Lamb and shear wave velocities was about 10% and 23% for Class 2 and Class 3 with respect to Class 1, respectively. This interesting observation was made despite the nonlinear relation between the Lamb and shear wave velocities, Eq. (1). It was also revealed that the standard deviation of the obtained Lamb wave velocities for each class was within 3% of the mean value, and thus not reported in this table. It proves the repeatability of the procedure for the Lamb wave velocity measurement for specimens with different MC. Another observation made through the results presented in Table 2 is that the imaginary part of the Lamb and shear wavenumbers increased with MC. It



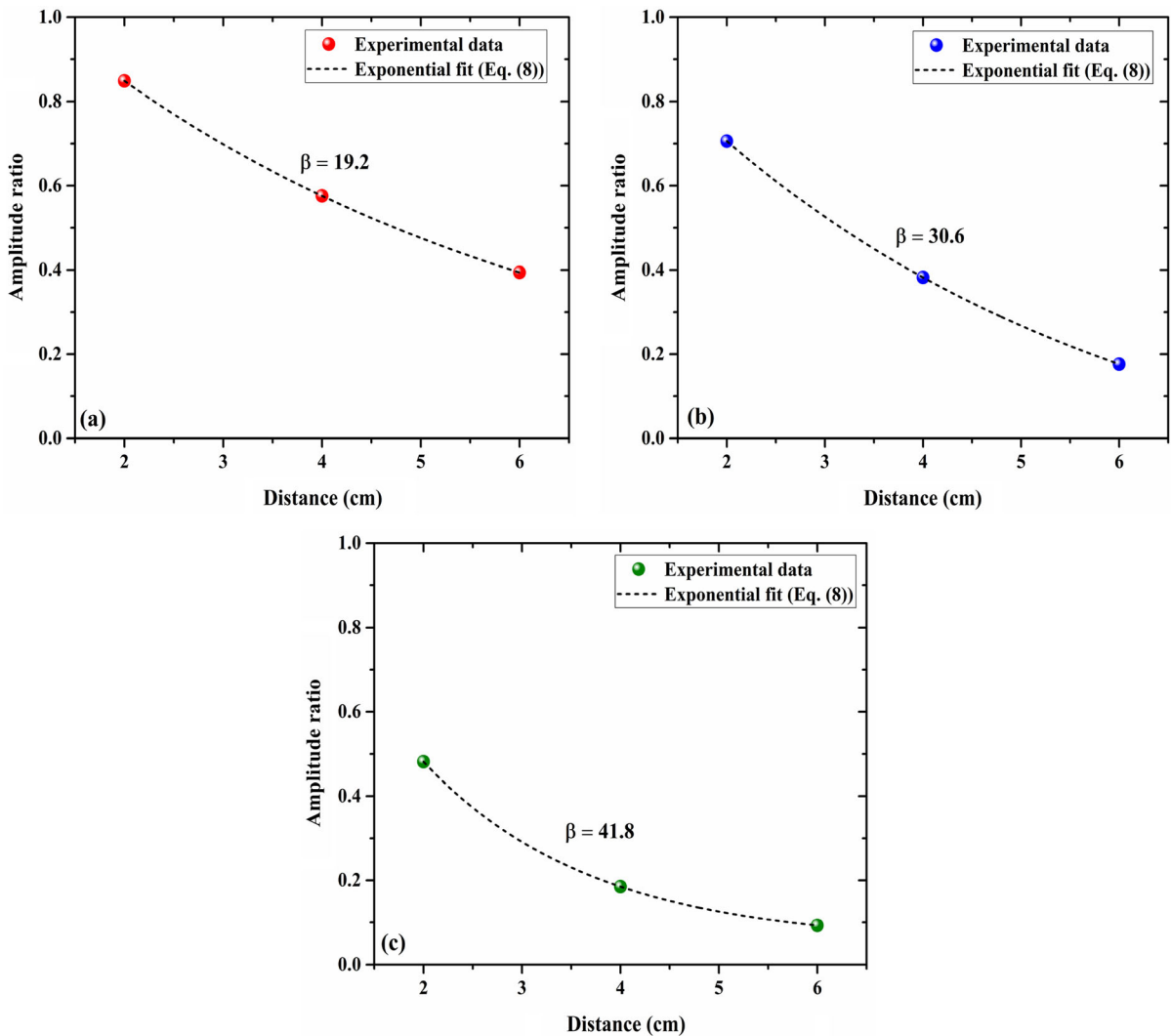


**Fig. 6** The Lamb wave amplitude ratio for **a** Class 1, **b** Class 2, and **c** Class 3 green poplar wood specimens. The distances given in the figure are those of each sensor from the first sensor at 6 cm

**Table 2** The Lamb and shear wave velocities and wavenumbers obtained through the Lamb wave propagation tests for different classes of green poplar wood specimens

Class	MC (%)	Lamb wave velocity (m/s)	Shear wave velocity (m/s)	Lamb wavenumber (rad/m)		Shear wavenumber (rad/m)	
		$c_l$	$c_s$	$\alpha_l$	$\beta_l$	$\alpha_s$	$\beta_s$
1	50–70	1743	1835	721	20.8	685	20.1
2	80–100	1568	1647	802	29.3	764	28.3
3	120–130	1341	1406	938	39.4	894	37.9



indicates that the viscoelasticity of the wood specimens increased with MC.

To the best of authors' knowledge, the Lamb wave propagation method has not been implemented for the characterization of wood materials in prior research studies, and thus the Lamb wave velocity in wood has not been reported. However, it was shown in the literature that the ultrasonic wave velocity decreased with MC [38, 39], while the correlation between the ultrasonic wave velocity and MC decreases at MC levels higher than the fiber saturation point (FSP), i.e.  $MC > 30\%$  [38]. The results presented in Table 2, however, revealed a high correlation between the Lamb wave velocity and the MC over a broad range of MC.

The mean and standard deviation of the viscoelastic properties of the green poplar wood specimens estimated using the Lamb wave propagation method are shown in Fig. 7 for different classes of MC. As seen in this figure, the shear storage modulus, considered as the shear stiffness of viscoelastic materials, decreased with MC, which indicates that the wood specimens were stiffer at lower MC. This is consistent with the observations made for the MOE of clear southern pine [40]. A similar trend was also reported for European beech wood [41]. It was also observed in Fig. 7 that the shear loss modulus and loss factor increased with MC. This indicates that the viscoelasticity of the green wood specimens increased with MC. The loss factor of the specimens, which is proportional to the ratio of the energy dissipated and the energy stored in a viscoelastic material during dynamic loading [35], was between 5.88% and 8.49%, which is higher than that for many viscoelastic polymers. Thus, the viscoelastic behavior of green wood is significant and cannot be neglected when investigating the mechanical properties and performance of wood structures. More interestingly, the difference between the loss factor of Class 1 and Class 3 wood specimens was as high as 44%, while such a difference for the shear storage and shear loss moduli was 14% and 25%, respectively. Therefore, it is concluded that the loss factor showed a higher sensitivity to the MC of the green wood specimens and may be used as an important mechanical property for the characterization and classification of wood. The viscoelastic properties of wood may be explained by the fact that wood has a poroelastic structure consisted of a porous solid matrix containing water. Such poroelastic

structures are known to dissipate energy and show viscoelastic behavior due to the interactions of the solid and fluid phases and the internal friction between them [42]. Consequently, the rate of the energy dissipation in wood, and thus its viscoelasticity increases with the MC.

The comparison between the elastic modulus of green poplar wood specimens obtained from the mechanical three-point bending tests ( $E_m$ ) and their elastic storage modulus estimated through the nondestructive Lamb wave propagation tests ( $E'_1$ ) is illustrated in Fig. 8. As observed in this figure, there was a good agreement between the results obtained from these two methods. The difference between the estimated results presented in Fig. 8 was smaller than 3% for different classes of MC. This minor discrepancy increased with MC, as at higher viscoelasticities the elastic modulus obtained based on the elastic assumption for the wood deviates more from the elastic storage modulus obtained based on the viscoelastic assumption [35]. It is also seen in Fig. 8 that the mechanical tests performed based on the elastic assumption slightly overestimated the stiffness of the wood specimens when compared with the elastic storage modulus obtained from the Lamb wave propagation method. A similar trend was reported in prior literature for other viscoelastic biomaterials [43]. Therefore, the Lamb wave propagation method not only yielded the shear loss modulus and the loss factor in addition to the shear storage modulus, but also improved the estimation of the stiffness (elastic storage modulus) of wood by considering it as a viscoelastic material and taking both of the real and imaginary parts of the Lamb wavenumber into account.

The results presented in this section confirmed the potential of the Lamb wave propagation method for accurate nondestructive estimation of the viscoelastic properties of wood materials with different MC. It was shown that the variations in the MC and material properties were captured in the Lamb wave characteristics, and thus the viscoelastic properties of wood specimens were reliably estimated. It provides this method with a great potential for in-situ monitoring and characterization of in-service structures. This study has limitations, such as the assumption of a macroscopically homogeneous and isotropic material for the propagation medium. The green wood



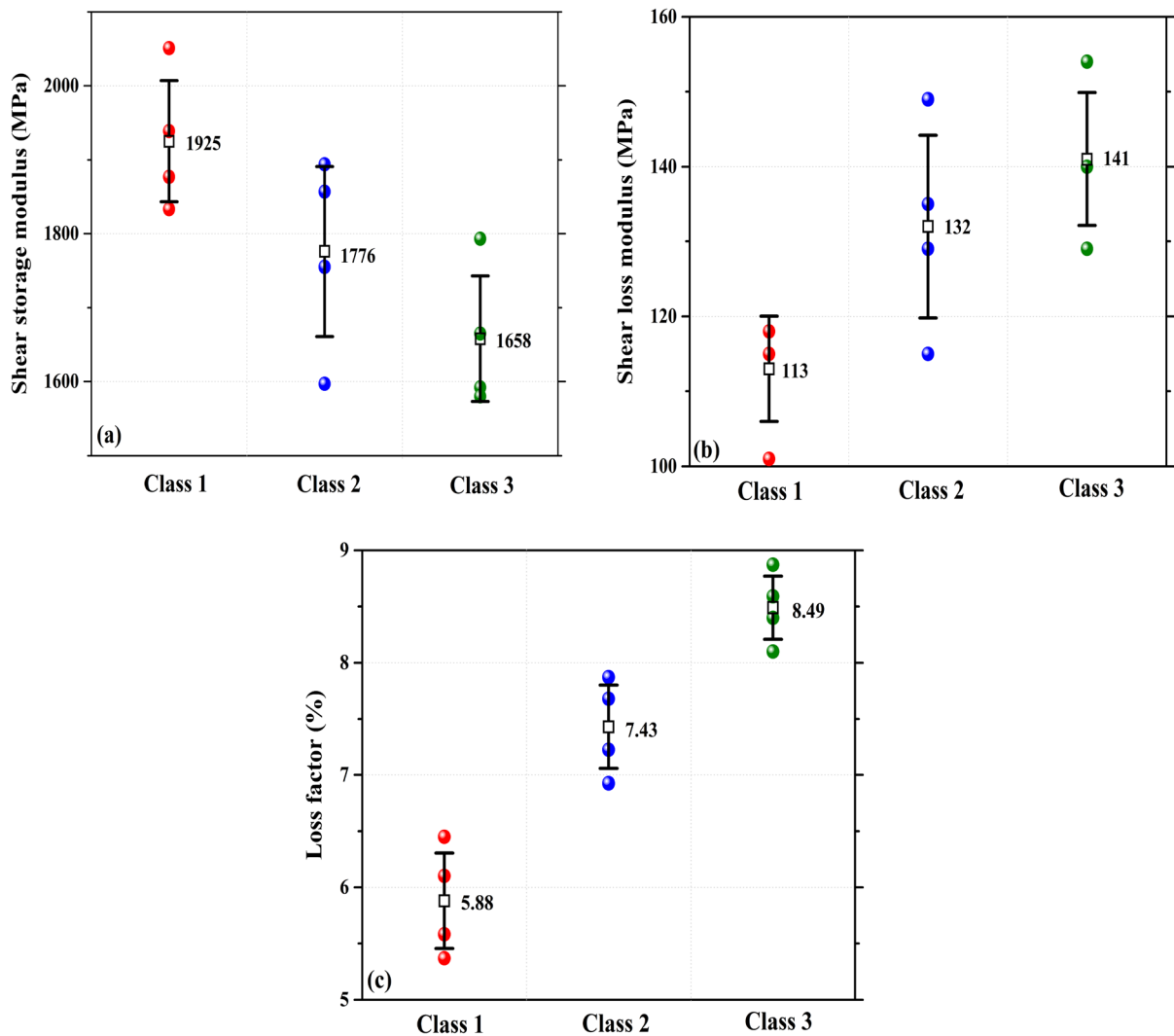


**Fig. 7** The mean and standard deviation of the viscoelastic properties of green poplar wood specimens including a the shear storage modulus, b shear loss modulus, and c loss factor for different classes of MC

specimens tested in this study showed an approximately homogeneous and isotropic behavior, as the measured Lamb wave velocity was nearly constant on the two L–T and L–R planes of each specimen. However, the further development of the Lamb wave propagation method for the characterization of the viscoelastic properties of anisotropic wood materials may be of interest for future work. Moreover, this method may be used for the viscoelasticity assessment of other types of bulk and composite wood materials in the future. As the sensitivity of the Lamb wave characteristics to tiny cracks and defects in a material is high, the potential of this method for damage

detection in wood materials and structures may also be investigated. Due to the low attenuation nature of guided Lamb waves, they can propagate over long distances in large structural timbers. Besides, the generation of the Lamb waves can be simply carried out using the contact or air-coupled transducers for such application. Therefore, the application of Lamb waves for the characterization and monitoring of large structural timbers may be properly carried out in future work. However, the test setup and excitation frequency may be slightly altered from that used in this study. For example, lower frequencies can be used for the characterization of large timbers to further decrease

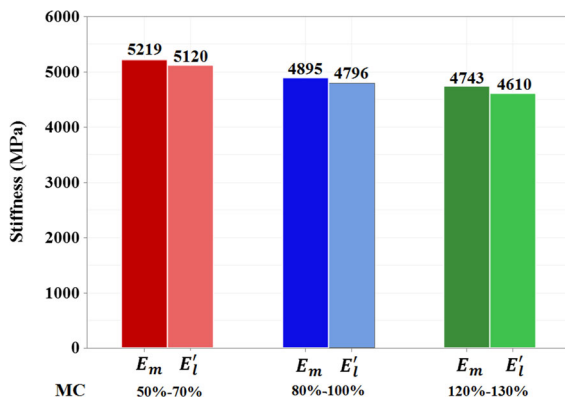


**Fig. 8** Comparison between the mean elastic modulus and elastic storage modulus of green poplar wood specimens with different MC obtained from the three-point bending and Lamb wave propagation tests, respectively

the Lamb wave attenuation, which causes the wave to propagate over longer distances. Furthermore, lower frequencies (higher wavelengths) result in the propagation of the guided waves deeper in the structure, which may be advantageous for damage detection purposes in large structures. Since structural timbers may contain defects such as knot, expanding the current study to cover defected specimens (i.e. including knot, etc.) may facilitate employing the Lamb wave propagation method to monitor structural timbers.

## 5 Conclusions

The moisture-dependent viscoelastic properties of wood materials were quantified using the nondestructive guided Lamb wave propagation method. The fundamental antisymmetric Lamb wave mode was propagated in the wood specimens, and the wave characteristics were obtained at several locations on the specimens along the propagation direction. The viscoelastic properties of the specimens with different MC were then obtained using the measured complex Lamb wavenumber and the estimated complex shear wavenumber. A high correlation was observed between the Lamb wave velocity and the viscoelastic properties of wood specimens estimated from the Lamb wave propagation method and the MC. The results showed that the tested wood specimens had significant viscoelasticity, which should be taken into account when assessing the mechanical properties of

wood materials for different engineering and structural applications. The shear storage modulus decreased and the loss factor increased with the MC, indicating that the structural stiffness and damping of wood and timber materials, respectively, decrease and increase with the MC. It was revealed that the sensitivity of the loss factor to the MC of the wood specimens was higher than that of the shear storage and shear loss moduli, suggesting that the loss factor can play an important role in the characterization and classification of wood materials. The elastic modulus of the specimens obtained from the three-point bending tests and their elastic storage modulus estimated through the Lamb wave propagation tests were in good agreement, where their difference was smaller at lower MC. It was shown that the elastic modulus obtained based on the elastic assumption for the wood may deviate from its real stiffness, especially at high MC levels. Therefore, it was concluded that it is of great importance to conduct the analysis of viscoelastic properties of wood, and the Lamb wave propagation method offers the potential for rapid and reliable nondestructive characterization of these properties at different MC level.

**Funding** This research study was not supported by any specific funding.

**Code availability** The MATLAB codes developed for the post-processing of the experimental data will be available upon reasonable request.

**Compliance with ethical standards**

**Availability of data and material** The experimental data of this study will be available if needed.

**Conflicts of interest** There are no known conflicts of interest associated with this manuscript.

## References

- Babiak M, Gaff M, Sikora A, Hysek Š (2018) Modulus of elasticity in three- and four-point bending of wood. *Compos Struct* 204:454–465. <https://doi.org/10.1016/j.compstruct.2018.07.113>
- Machado JS, Pereira F, Quilhó T (2019) Assessment of old timber members: Importance of wood species identification and direct tensile test information. *Constr Build Mater* 207:651–660. <https://doi.org/10.1016/j.conbuildmat.2019.02.168>



3. Riggio M, Anthony RW, Augelli F, Kasal B, Lechner T, Muller W, Tannert T (2014) In situ assessment of structural timber using non-destructive techniques. *Mater Struct Constr* 47:749–766. <https://doi.org/10.1617/s11527-013-0093-6>
4. Sandak J, Sandak A, Riggio M (2015a) Multivariate analysis of multi-sensor data for assessment of timber structures: principles and applications. *Constr Build Mater* 101:1172–1180. <https://doi.org/10.1016/j.conbuildmat.2015.06.062>
5. Ranta-Maunus A (1975) The viscoelasticity of wood at varying moisture content. *Wood Sci Technol* 9:189–205. <https://doi.org/10.1007/BF00364637>
6. Ranta-Maunus A (1993) Rheological behaviour of wood in directions perpendicular to the grain. *Mater Struct* 26:362–369. <https://doi.org/10.1007/BF02472962>
7. Placet V, Passard J, Perré P (2008) Viscoelastic properties of wood across the grain measured under water-saturated conditions up to 135 °C: evidence of thermal degradation. *J Mater Sci* 43:3210–3217. <https://doi.org/10.1007/s10853-008-2546-9>
8. Hering S, Niemz P (2012) Moisture-dependent, viscoelastic creep of European beech wood in longitudinal direction. *Eur J Wood Wood Prod* 70:667–670. <https://doi.org/10.1007/s00107-012-0600-4>
9. Dubois F, Husson JM, Sauvat N, Manfoumbi N (2012) Modeling of the viscoelastic mechano-sorptive behavior in wood. *Mech Time-Depend Mater* 16:439–460. <https://doi.org/10.1007/s11043-012-9171-3>
10. Ozyhar T, Hering S, Niemz P (2013) Viscoelastic characterization of wood: time dependence of the orthotropic compliance in tension and compression. *J Rheol (N Y N Y)* 57:699–717. <https://doi.org/10.1122/1.4790170>
11. Karaduman Y, Sayeed MMA, Onal L, Rawal A (2014) Viscoelastic properties of surface modified jute fiber/polypropylene nonwoven composites. *Compos Part B Eng* 67:111–118. <https://doi.org/10.1016/j.compositesb.2014.06.019>
12. Li Z, Jiang J, Lyu J (2019) Moisture-dependent orthotropic viscoelastic properties of Chinese fir wood during quenching in the temperature range of 20 to –120 °C. *Holzforchung*. <https://doi.org/10.1515/hf-2018-0281>
13. Wouts J, Haugou G, Oudjene M, Coutellier D, Morvan H (2016) Strain rate effects on the compressive response of wood and energy absorption capabilities—Part A: experimental investigations. *Compos Struct* 149:315–328. <https://doi.org/10.1016/j.compstruct.2018.07.001>
14. Riggio M, Sandak J, Sandak A, Pauliny D, Babiński L (2014) Analysis and prediction of selected mechanical/dynamic properties of wood after short and long-term water-logging. *Constr Build Mater* 68:444–454. <https://doi.org/10.1016/j.conbuildmat.2014.06.085>
15. Sandak A, Sandak J, Riggio M (2015b) Estimation of physical and mechanical properties of timber members in service by means of infrared spectroscopy. *Constr Build Mater* 101:1197–1205. <https://doi.org/10.1016/j.conbuildmat.2015.06.063>
16. Nasir V, Nourian S, Zhou Z, Rahimi S, Avramidis S, Cool J (2019) Classification and characterization of thermally modified timber using visible and near-infrared spectroscopy and artificial neural networks: a comparative study on the performance of different NDE methods and ANNs. *Wood Sci Technol* 53:1093–1109. <https://doi.org/10.1007/s00226-019-01120-0>
17. Beall FC (2002) Overview of the use of ultrasonic technologies in research on wood properties. *Wood Sci Technol* 36:197–212. <https://doi.org/10.1007/s00226-002-0138-4>
18. García-Iruela A, Fernández FG, Esteban LG, De Palacios P, Simón C, Arriaga F (2016) Comparison of modelling using regression techniques and an artificial neural network for obtaining the static modulus of elasticity of *Pinus radiata* D. Don. timber by ultrasound. *Compos Part B Eng* 96:112–118. <https://doi.org/10.1016/j.compositesb.2016.04.036>
19. Morales-Conde MJ, Rodríguez-Liñán C, Rubio-de Hita P (2016) A study of the wood-related factors involved in non-destructive ultrasound tests perpendicular to the grain for Scots pine. *Mater Struct* 49:1543–1552. <https://doi.org/10.1617/s11527-015-0594-6>
20. Nasir V, Nourian S, Avramidis S, Cool J (2019a) Stress wave evaluation for predicting the properties of thermally modified wood using neuro-fuzzy and neural network modeling. *Holzforchung* 73:827–838. <https://doi.org/10.1515/hf-2018-0289>
21. Nasir V, Nourian S, Avramidis S, Cool J (2019b) Stress wave evaluation by accelerometer and acoustic emission sensor for thermally modified wood classification using three types of neural networks. *Eur J Wood Wood Prod* 77:45–55. <https://doi.org/10.1007/s00107-018-1373-1>
22. Bouhamed N, Souissi S, Marechal P, Amar MB, Lenoir O, Leger R, Bergeret A (2020) Ultrasound evaluation of the mechanical properties as an investigation tool for the wood-polymer composites including olive wood flour. *Mech Mater*. <https://doi.org/10.1016/j.mechmat.2020.103445>
23. Ettelaei A, Layeghi M, Zarea Hosseinabadi H, Ebrahimi G (2019) Prediction of modulus of elasticity of poplar wood using ultrasonic technique by applying empirical correction factors. *Meas J Int Meas Confed* 135:392–399. <https://doi.org/10.1016/j.measurement.2018.11.076>
24. Lee CJ, Wang SY, Yang TH (2011) Evaluation of moisture content changes in Taiwan red cypress during drying using ultrasonic and tap-tone testing. *Wood Fiber Sci* 43:57–63
25. Baar J, Tippner J, Rademacher P (2015) Prediction of mechanical properties—modulus of rupture and modulus of elasticity—of five tropical species by nondestructive methods. *Maderas Cienc y Tecnol* 17:239–252. <https://doi.org/10.4067/S0718-221X2015005000023>
26. Chauhan S, Sethy A (2016) Differences in dynamic modulus of elasticity determined by three vibration methods and their relationship with static modulus of elasticity. *Maderas Cienc y Tecnol* 18:373–382. <https://doi.org/10.4067/S0718-221X2016005000034>
27. Dahmen S, Ketata H, Ben Ghazlen MH, Hosten B (2010) Elastic constants measurement of anisotropic Olivier wood plates using air-coupled transducers generated Lamb wave and ultrasonic bulk wave. *Ultrasonics* 50:502–507. <https://doi.org/10.1016/j.ultras.2009.10.014>
28. Chow G, Uchaker E, Cao G, Wang J (2015) Laser-induced surface acoustic waves: an alternative method to nanoindentation for the mechanical characterization of porous nanostructured thin film electrode media. *Mech Mater* 91:333–342. <https://doi.org/10.1016/j.mechmat.2015.10.005>





29. Yang B, Xuan FZ, Chen S, Zhou S, Gao Y, Xiao B (2017) Damage localization and identification in WGF/epoxy composite laminates by using Lamb waves: experiment and simulation. *Compos Struct* 165:138–147. <https://doi.org/10.1016/j.compstruct.2017.01.015>
30. Duan W, Gan TH (2019) Investigation of guided wave properties of anisotropic composite laminates using a semi-analytical finite element method. *Compos Part B Eng* 173:106898. <https://doi.org/10.1016/j.compositesb.2019.106898>
31. Mardanshahi A, Nasir V, Kazemirad S, Shokrieh MM (2020) Detection and classification of matrix cracking in laminated composites using guided wave propagation and artificial neural networks. *Compos Struct* 246:112403. <https://doi.org/10.1016/j.compstruct.2020.112403>
32. Mardanshahi A, Shokrieh MM, Kazemirad S (2020) Identification of matrix cracking in cross-ply laminated composites using Lamb wave propagation. *Compos Struct* 235:111790. <https://doi.org/10.1016/j.compstruct.2019.111790>
33. Kundu T (2003) *Ultrasonic nondestructive evaluation: engineering and biological material characterization*. CRC Press, Boca Raton
34. Fathi H, Nasir V, Kazemirad S (2020) Prediction of the mechanical properties of wood using guided wave propagation and machine learning. *Constr Build Mater* 262:120848. <https://doi.org/10.1016/j.conbuildmat.2020.120848>
35. Lakes R (2009) *Viscoelastic materials*. Cambridge University Press, Cambridge. <https://doi.org/10.1017/CBO9780511626722>
36. Gonçalves R, Trinca AJ, Cerri DGP (2011) Comparison of elastic constants of wood determined by ultrasonic wave propagation and static compression testing. *Wood Fiber Sci* 43:64–75
37. Green DW, Winandy JE, Kretschmann DE (1999) *Mechanical properties of wood*. Wood handbook: wood as an engineering material. USDA Forest Service Forest Products Laboratory, Madison, WI
38. Jiang J, Bachtiar EV, Lu J, Niemz P (2018) Comparison of moisture-dependent orthotropic Young's moduli of Chinese fir wood determined by ultrasonic wave method and static compression or tension tests. *Eur J Wood Wood Prod* 76:953–964. <https://doi.org/10.1007/s00107-017-1269-5>
39. Yang H, Yu L, Wang L (2015) Effect of moisture content on the ultrasonic acoustic properties of wood. *J For Res* 26:753–757. <https://doi.org/10.1007/s11676-015-0079-z>
40. Kretschmann DE, Green DW (1996) Modeling moisture content-mechanical property relationships for clear southern pine. *Wood Fiber Sci* 28:320–337
41. Ozyhar T, Hering S, Niemz P (2012) Moisture-dependent elastic and strength anisotropy of European beech wood in tension. *J Mater Sci* 47:6141–6150. <https://doi.org/10.1007/s10853-012-6534-8>
42. Biot MA (1962) Mechanics of deformation and acoustic propagation in porous media. *J Appl Phys* 33:1482–1498. <https://doi.org/10.1063/1.1728759>
43. Kazemirad S, Bernard S, Hybois S, Tang A, Cloutier G (2016) Ultrasound shear wave viscoelastography: model-independent quantification of the complex shear modulus. *IEEE Trans Ultrason Ferroelectr Freq Control* 63:1399–1408. <https://doi.org/10.1109/TUFFC.2016.2583785>

**Publisher's Note** Springer Nature remains neutral with regard to jurisdictional claims in published maps and institutional affiliations.

